ISSN: 0067-2904

Electron Scattering from Stable and Exotic Li Isotopes

Ameen M. Hameed*, Arkan R. Ridha
Department of Physics, College of Science, University of Baghdad, Baghdad, Iraq

Received: 29/11/2022 Accepted: 3/4/2023 Published: 30/3/2024

Abstract

The nuclear shell model was used to investigate the bulk properties of lithium isotopes (^{6,7,8,9,11}Li), i.e., the ground state density distributions and C0 and C2 components of charge form factors. The theoretical treatment was based on supposing that the Harmonic-oscillator (HO) potential governs the core nucleons while the valence nucleon(s) move through Hulthen potential. Such assumptions were applied for both stable and exotic lithium isotopes. The HO size parameters (b_n and b_p), the core radii (r_c) and the attenuation parameters (κ_n and κ_p) were fixed to recreate the available empirical size radii for lithium isotopes under study.

Keywords: size radii, density distributions, electron scattering charge form factors, exotic nuclei, shell model, Lithium isotopes, Hulthen potential

الاستطارة الالكترونية من نظائر الليثيوم المستقرة والغريبة

امين مطاع حميد*، أركان رفعه رضا
قسم الفيزياء, كلية العلوم, جامعة بغداد, محافظة بغداد, العراق

الخلاصة:

تم استخدام انموذج القشرة النووي لتحقيق الخصائص الحجمية لنظائر الليثيوم (^{6,7,8,9,11}Li)، أي توزيعات كثافة الحالة الأرضية والمركبات C0 و C2 لعوامل التشكيل الشحنية. استندت المعالجة النظرية إلى افتراض أن جهد المذبذب التوافقي (HO) يتحكم في نيوكليونات القلب، بينما تتحرك نيوكليونات التكافؤ تحت جهد هالثين. تم تطبيق هذا الافتراض او المعالجة لكلاً من نظائر الليثيوم المستقرة والغريبة. معلمات جهد المتذبذب التوافقي و وانصاف اقطار القلب و معامل التوهين لكلا من البروتونات والنيوترونات ثبتت بحيث تعيد توليد انصاف الاقطار المتوفرة عمليا لنظائر الليثيوم تحت الدراسة.

Introduction

The advent of radioactive ion beam facilities and the discovery of exotic nuclei in the mid-1980s by Anahita et al. [1] opened a new branch in nuclear physics studied through new modified theoretical models. An excess in the number of neutrons or protons distinguish these nuclei. One of the outstanding properties of exotic nuclei is the halo phenomenon, mainly characterized by the appearance of a long tail at large r in the density distribution. Such a tail is needed to explain the large reaction cross-section for some neutron-rich nuclei [2]. Therefore, the regeneration of the long tail at large r is important. The Gaussian downfall behavior is the main reason the Harmonic-Oscillator Wave Functions (HOWFs) do not give satisfactory results

[3,4,5]. Several methods were used to study the stable and the exotic nuclei, such as using two HO size parameters: one for the core and the other for the halo part [6,7]. The transformed HOWFs (THO) in the local scale transformation [8,9] are also researched. The Woods-Saxon and Cosh potentials were applied with very good results to study some light stable, and exotic nuclei [10,11].

In this paper, the radial WF of $1s_{\frac{1}{2}}$ of Hulthen potential was used to describe the valance nucleon(s) of all studied lithium isotopes, while the core nucleons were studied using HOWFs. With such modification, the size radii, density distributions and charge form factors of stable and exotic lithium isotopes were calculated.

Theoretical Formulations

The radial part of the second order Schrödinger differential equation is given by [12]:

$$\frac{1}{r^2}\frac{d}{dr}\left(r^2\frac{d\emptyset_{nlj,t_z}(r)}{dr}\right)+\frac{2\mu_{cm_{t_z}}}{\hbar^2}\left[E_{t_z}-\frac{l(l+1)\hbar^2}{2mr^2}-U(r)\right]\emptyset_{nlj,t_z}(r)=0 \quad (1)$$

The n, l, j, t_z ($t_z=\frac{1}{2}$ for proton and $t_z=-\frac{1}{2}$ for neutron), μ and $\hbar$ represent principle, orbital, total spin and total isospin for single nucleon, reduced mass ($\mu_{cm_{t_z}}=\frac{m_{t_z}m_c}{A}$) and Planck's constant, respectively. The binding energy and separation energy of single proton or neutron are represented by E_{t_z} and S_{t_z} ($E_{t_z}=-S_{t_z}$), respectively in Eq. (1). $U(r)$ represents the nuclear central potential given for Hulthen mean field in the form [13]:

$$U(r)=U^H_{cm_{t_z}}(r)=\frac{V_{0,t_z}}{(e^{\beta_{t_z}r}-1)} \quad (2)$$

The range of the potential R is related to β_{t_z} by the formula $\beta_{t_z}=\frac{1}{R}$, besides, V_0 represent the depth of the potential. The only s state solution to Eq. (1) is given analytically as [13,14]:

$$\emptyset_{nlj,t_z}(r)=\frac{S_{i,t_z}(r)}{r}\,Y_{00}(\hat{r}) \quad (3)$$

In Eq. (3), the $S_i(r)$ is the radial form of Weinberg states and $Y_{00}(\hat{r})$ is the spherical harmonics. Knowing that $S_i(r)$ is given by [13, 14]:

$$S_{i,t_z}(r)=e^{-\kappa_{t_z}r}\sum_{j=0}^{i}a^{(i)}_{j,t_z}e^{-j\beta_{t_z}r} \quad (4)$$

$a^{(i)}_{j,t_z}$ satisfies the condition and the recurrence relation given by [13,14]:

$$\sum_{j=0}^{i}a^{(i)}_{j,t_z}=0 \quad (5)$$

and

$$\alpha^{(i)}_{j+1,t_z}=\alpha^{(i)}_{j,t_z}\left(\frac{j\omega_{1,t_z}-\omega_{i,t_z}+j(j-1)}{(j+1)(j+\omega_{1,t_z})}\right) \quad (6)$$

where

$$\omega_{i,t_z}=-\alpha_{i,t_z}\left(\frac{2\mu_{cm_{t_z}}V_{0,t_z}}{\hbar^2\beta^2_{t_z}}\right) \quad (7)$$

The parameters of Weinberg state (α_{i,t_z}) are given by [13,14]:

$$\alpha_{i,t_z} = i\left(\frac{2\kappa_{t_z} + i\beta_{t_z}}{2\kappa_{t_z} + \beta_{t_z}}\right) \tag{8}$$

In Eq. (3), the $1s_{\frac{1}{2}}$ state denoted by $\emptyset_{1s_{\frac{1}{2}},t_z}(r)$ can be written with the aid of Eqs. 4 to 8 as:

$$\emptyset_{1s_{\frac{1}{2}},t_z}(r) = \frac{\sqrt{2\kappa_{t_z}(\kappa_{t_z} + \beta_{t_z})(2\kappa_{t_z} + \beta_{t_z})}}{\beta_{t_z}} \frac{e^{-\kappa_{t_z} r}}{r}[1 - e^{-\beta_{t_z} r}]Y_{00}(\hat{r}) \tag{9}$$

The wave number κ_{t_z} is related to the binding energy of the single proton (neutron) by:

$$\kappa_{t_z}^2 = \frac{2\mu_{cm_{t_z}} S_{t_z}}{\hbar^2} \tag{10}$$

The depth of the potential has a relationship with β_{t_z} and κ_{t_z} by:

$$V_{0,t_z} = -\frac{\hbar^2 \beta_{t_z}^2}{2\mu_{cm_{t_z}}}\left(1 + \frac{2\kappa_{t_z}}{\beta_{t_z}}\right) \tag{11}$$

For HO potential, where in Eq. (1), $U(r) = -V_0 + \frac{1}{2} m_{t_z} \omega^2 r^2$, the radial WF is given by [15]:

$$R_{nl}(r, b_{t_z}) = \frac{1}{(2l+1)!!}\left[\frac{2^{l-n+3}(2n+2l-1)!!}{\sqrt{\pi} b_{t_z}^3 (n-1)!}\right]^{\frac{1}{2}} \left(\frac{r}{b_{t_z}}\right)^l e^{-\frac{r^2}{2b_{t_z}^2}} \sum_{k=0}^{n-1}(-1)^k \frac{(n-1)!2^k(2l+1)!!}{(n-k-1)!k!(2l+2k+1)} \left(\frac{r}{b_{t_z}}\right)^{2k} \tag{12}$$

where b_{t_z} stands for the HO size parameter for neutrons or protons.

The density distributions of protons and neutrons for neutron rich isotopes can be written as:

$$\rho_p(r) = \frac{1}{4\pi} \sum_{c \in core} n_{c,p} \left|R_{n_c l_c}(r, b_p)\right|^2 \tag{13}$$

$$\rho_n(r) = \frac{1}{4\pi} \sum_{c \in core} n_{c,n} \left|R_{n_c l_c}(r, b_n)\right|^2 + \frac{1}{4\pi} n_{v,n} \left|\emptyset_{1s_{\frac{1}{2}},n}(r)\right|^2 \tag{14}$$

In the above two equations, n_{c,t_z} is the number of protons (neutrons) in the core (c) shells.

The $n_{v,n}$ represents the number of neutron(s) in the valence part.

The density distributions of protons and neutrons for proton rich isotopes can be written as:

$$\rho_n(r) = \frac{1}{4\pi} \sum_{c \in core} n_{c,n} \left|R_{n_c l_c}(r, b_n)\right|^2 \tag{15}$$

$$\rho_p(r) = \frac{1}{4\pi} \sum_{c \in core} n_{c,p} \left|R_{n_c l_c}(r, b_p)\right|^2 + \frac{1}{4\pi} n_{v,p} \left|\emptyset_{1s_{\frac{1}{2}},p}(r)\right|^2 \tag{16}$$

where $n_{v,p}$ is the number of neutron (s) in the valence part.

The density distributions of protons and neutrons for stable ^{6}Li and ^{7}Li nuclei can be written as:

$$\rho_{t_z}(r) = \frac{1}{4\pi} \sum_{c \in core} n_{c,t_z} \left|R_{n_c l_c}(r, b_{t_z})\right|^2 + \frac{1}{4\pi} n_{v,t_z} \left|\emptyset_{1s_{\frac{1}{2}},t_z}(r)\right|^2 \tag{17}$$

The Charge Density Distribution (CDD) can be accounted by folding the point proton and neutron density distribution to the CDD of single proton and neutron following the procedure of Ridha and Abbas [16]:

$$\rho_{ch}(r) = \rho_{ch,p}(r) + \rho_{ch,n}(r) \tag{18}$$

where

$$\rho_{ch,p}(r) = \int \rho_p(r)\rho_{pr}(\boldsymbol{r}-\boldsymbol{r'})d\boldsymbol{r'} \tag{19}$$

and

$$\rho_{ch,n}(r) = \int \rho_{J=0,n}(r)\rho_{neu}(\boldsymbol{r}-\boldsymbol{r'})d\boldsymbol{r'} \tag{20}$$

The size radii (root mean square (rms) proton, neutron, charge and matter) are evaluated [17]:

$$\langle r^2\rangle_i^{\frac{1}{2}} = \sqrt{\frac{4\pi}{i}\int_0^\infty \rho_i(r)r^4dr} \tag{21}$$

where i stands for the proton, neutron, charge and matter.

Finally, the charge form factors in the plane-wave Born approximation is given by [17]:

$$F_{ch}^J(q) = \frac{4\pi}{qZ}\int_0^\infty \rho_{ch}^J(r)\sin(qr)\,rdr \tag{22}$$

where q and Z represent the momentum transferred to the nucleus from incident electrons and the atomic number of the target nucleus, respectively.

$$\rho_{ch}^J(r) = \rho_{ch,CP}^J(r) + \rho_{ch,MS}^J(r) \tag{23}$$

Two mathematical forms of CP were chosen, the Bohr-Mottelson [18] and Tassie [19] models, given respectively by:

$$\rho_{ch,T}^J(r) = N_T r^{J-1}\frac{d\rho_{ch}(r)}{dr} \tag{24}$$

and

$$\rho_{ch,BM}^J(r) = N_{BM}\frac{d\rho_{ch}(r)}{dr} \tag{25}$$

In Eq. (23), the model space (MS) contribution is accounted from shell model calculations by: [6]

$$\rho_{MS}^J(r) = \frac{1}{\sqrt{4\pi}}\frac{1}{\sqrt{2J_i+1}}\sum_{ab} X_{a,b,t_z}^{J_f\ J_i\ J}\left\langle j_a\middle\|Y_J\middle\|j_b\right\rangle R_{n_a l_a j_a,t_z}(r)R_{n_b l_b j_b,t_z}(r) \tag{26}$$

In Eq. (24) and (25), the normalization constants are chosen so as to regenerate the experimental reduced transition probability:

$$N_T = \frac{\sqrt{(2J_i+1)B\left(EJ,J_i\to J_f\right)} - \int_0^\infty r^{J+2}\rho_{ch,MS}^J(r)dr}{\int_0^\infty r^{2J+1}\frac{d\rho_{ch}(r)}{dr}dr} \tag{27}$$

$$N_{BM} = \frac{\sqrt{(2J_i+1)B\left(EJ,J_i\to J_f\right)} - \int_0^\infty r^{J+2}\rho_{ch,MS}^J(r)dr}{\int_0^\infty r^{J+1}\frac{d\rho_{ch}(r)}{dr}dr} \tag{28}$$

The experimental reduced transition probability is related to experimental quadrupole moment by the relation:

$$B\left(EJ,J_i\to J_f\right) = \frac{5Q^2}{(2J_i+1)16\pi\begin{pmatrix} J & 2 & J \\ -J & 0 & J\end{pmatrix}^2} \tag{23}$$

Results and Discussion

In the present work, the nuclear shell model was adopted to describe the core and valence nucleons for lithium isotopes (^{6,7,8,9,11}Li). For ^{6,7}Li, the configuration interaction was chosen. The nuclear shell model code oxbash was operated to start the calculations using the Cohen-Kurath interaction (CKI) [20] in the p shell. The HO was used for the core ^{4}He while the HO and Hulthen WFs were used for 1p-shell model space. For ^{8,9,11}Li, the pure configuration was adopted. The parameters of HO and Hulthen potentials were fixed to generate the available size radii for all studied lithium isotopes (^{6,7,8,9,11}Li).

In Table 1, the parameters J^{π}, $t_{1/2}$, b_c and κ_{t_z} represent the total spin and parity, the half-life, the HO size parameters for protons and neutrons in the core, the attenuation parameter for proton and neutron and finally the experimental binding energy for single protons and neutrons on Fermi's level, respectively. From Eq. (10), the experimental binding energies of the single proton (S_p) and neutron (S_n) were used to calculate the attenuation parameter for the proton and neutron. The size radii for nuclei under study was reproduced using the adjustable $b_{c,n}$and $b_{c,p}$ parameters.

In Table 2, the computed size radii (charge $\langle r^2\rangle_{ch}^{1/2}$, proton $\langle r^2\rangle_{p}^{1/2}$, neutron $\langle r^2\rangle_{n}^{1/2}$ and matter $\langle r^2\rangle_{m}^{1/2}$) for ^{6,7,8,9,11}Li isotopes are shown. The calculated data were compared with the available experimental data. It is obvious that the results agreed with empirical data.

The computed CDD and charge form factors for C0 + C2 for ^{6}Li and ^{7}Li are drawn in Figure1(a), (b), (c) and (d), respectively. The occupation numbers in s-p-shell for ^{6}Li adjusted for neutrons $n_{1s_{\frac{1}{2}},n} = 1.9$ and $n_{1p,n} = 0.1$ and $n_{v,n} = 1$ and protons are $n_{1s_{\frac{1}{2}},p} = 1.2$ and $n_{1p,p} = 0.3$ and $n_{v,p} = 1.5$, respectively. The occupation numbers in s-p-shell for ^{7}Li adjusted for neutrons $n_{1s_{\frac{1}{2}},n} = 2$ and $n_{1p,n} = 0.5$ and $n_{v,n} = 1.5$ and protons are $n_{1s_{\frac{1}{2}},p} = 1.25$ and $n_{1p,p} = 0.6$ and $n_{v,p} = 1.15$, respectively. The calculated CDD in

Figure1(a) and (c) are in perfect agreement with the experimental data [21]. In Figure1(b) and (d) the calculated charge form factors are calculated by taking into consideration the contributions from model space and CP. The model space contribution was accounted using the configuration mixing using CKI interaction [20]. The CP was calculated using Bohr Mottelson (solid curves) and Tassie (short dashed curves) models. It is clear that the theoretical predictions of Bohr Mottelson model are in good agreement with the experimental data; in contrast, Tassie model highly underestimated the results at medium and large q. The normalization constant in Eq. (27) and (28) were selected to regenerate the quadrupole moment for ^{6}Li $Q_{exp.} = -0.082\ efm^2$ [22] and for ^{7}Li $Q_{exp.} = -4.06\ efm^2$[22].

In Figure 2(a), (b) and (c), the calculated MDDs for ^{8,9,11}Li are shown. The theoretical calculations using the radial wave functions of HO and Hulthen potentials are denoted by solid curves denoted by HO+Hulthen. The shaded areas represent the empirical data. It is obvious the appearance of the long tail in all figures, which is the main feature of halo nuclei. This makes it obvious the excellent agreement with the experimental data.

Figure3 shows the calculated MDDs for (^{6,7,8,9,11}Li). The long tail behavior appears for (^{8,9,11}Li) more than (^{6,7}Li) because the increase in the number of neutrons decreases the binding energy of the last neutron, and the increase in the tunnelling effect lead to the halo formation.

The calculated Coulomb form factors for (^{6,7,8,9,11}Li) nuclei are depicted in Figure 4. With the increase of the neutron number, the charge form factors are shifted forwards and upwards leading to an increase in the scattering process due to the screening effect.

Table 1: $J^{\pi}T$, $t_{1/2}$, $b_{c,n}$, $b_{c,p}$, κ_n ,κ_p , S_p and S_n for lithium (^{6,7,8,9,11}Li) isotopes

$^{A}_{Z}X_N(J^{\pi}T)$ [23]	$t_{\frac{1}{2}}(ms)$ [23]	$b_{c,n}$and $b_{c,p}$	κ_n and κ_p	Exp. Neutron binding energy (MeV) [24]	Exp. Proton binding energy (MeV) [24]
$^{6}Li(1^{+}0)$	Stable	$b_{c,n} = 1.67$ $b_{c,p} = 1.649$	$\kappa_n = 0.477$ $\kappa_p = 0.490$	$S_n = 5.6633245 \pm 0.05$	$S_p = 4.4333246 \pm 0.02$
$^{7}Li\left(\frac{3}{2}^{-}\ \frac{1}{2}\right)$	Stable	$b_{c,n} = 1.75$ $b_{c,p} = 1.73$	$\kappa_n = 0.642$ $\kappa_p = 0.680$	$S_n = 7.2510939 \pm 0.0000045$	$S_p = 9.9739616 \pm 0.0000531$
$^{8}Li(2^{+}1)$	838.7 ± 0.0003	$b_{c,n} = 1.65$ $b_{c,p} = 1.63$	$\kappa_n = 0.293$	$S_n = 2.0326182 \pm 0.0000472$	$S_p = 12.4162941 \pm 0.0075596$
$^{9}Li\left(\frac{3}{2}^{-}\ \frac{3}{2}\right)$	178.2 ± 0.0004	$b_{c,n} = 1.6$ $b_{c,p} = 1.545$	$\kappa_n = 0.417$	$S_n = 4.0622175 \pm 0.0001922$	$S_p = 13.9437489 \pm 0.0002064$
$^{11}Li\left(\frac{3}{2}^{-}\ \frac{5}{2}\right)$	8.75 ± 0.00006	$b_{c,n} = 1.78$ $b_{c,p} = 1.77$	$\kappa_n = 0.132$	$S_n = 0.3956871 \pm 0.0127362$	$S_p = 15.7578592 \pm 0.0928497$

Table 2: Computed and experimental rms charge, proton, neutron and matter radii for Lithium (^{6,7,8,9,11}Li).

$^{A}_{Z}X_N(J^{\pi}T)$ [23]	Calculate $\langle r^2\rangle_n^{1/2}$	Exp. $\langle r^2\rangle_n^{1/2}$	Calculate $\langle r^2\rangle_p^{1/2}$	Exp. $\langle r^2\rangle_p^{\frac{1}{2}}$	Calculate $\langle r^2\rangle_m^{1/2}$	Exp. $\langle r^2\rangle_m^{1/2}$	Calculate $\langle r^2\rangle_{ch}^{1/2}$	Exp. $\langle r^2\rangle_{ch}^{1/2}$
^{6}Li	2.297	2.27(7)[25]	2.486	2.45(4)[26]	2.393	2.44(7)[26]	2.588	2.56(5)[27]
^{7}Li	2.386	2.39(4)[25]	2.326	-	2.360	2.38(3)[28]	2.426	2.41(10)[21]
^{8}Li	2.551	2.66(11)[26]	2.207	2.20(5)[26]	2.428	2.45(6)[29]	2.305	2.299(32)[30]
^{9}Li	2.417	2.43(3)[25]	2.092	2.076 ± 0.037 [25]	2.314	2.32(2)[31]	2.186	2.217(35)[30]
^{11}Li	3.337	3.36(38)[25]	2.396	2.358 ± 0.039 [25]	3.109	3.12(30)[32	2.468	2.467(37)[30]

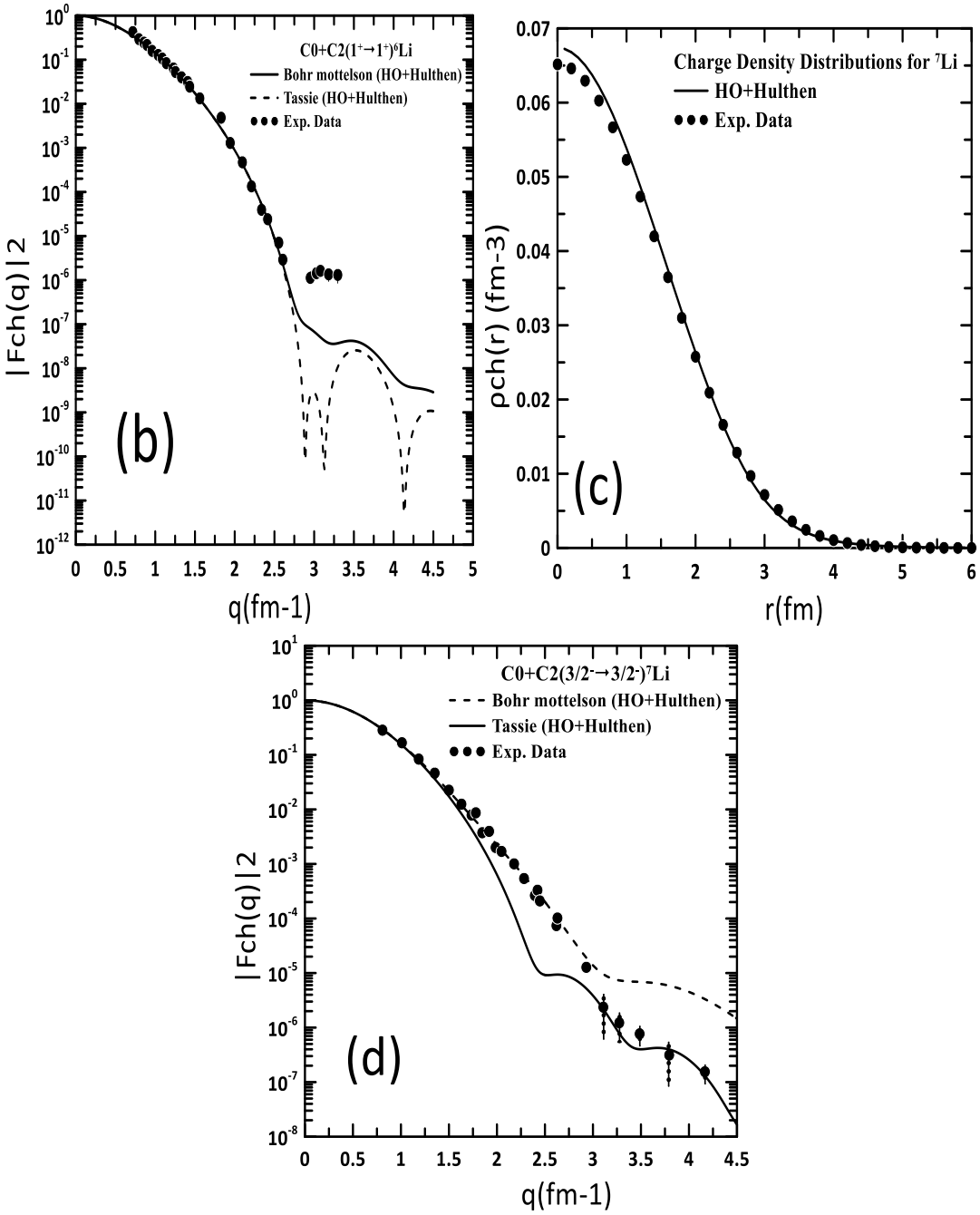

Figure 1: (a), (b), (c) and (d): The theoretical results indicated by the solid curves (HO+H). The doted symbols represented the experimental data [21] for the CDDs of ^{6,7}Li and the C0+C2 charge form factor for ^{6}Li [33] and for ^{7}Li [34,35].

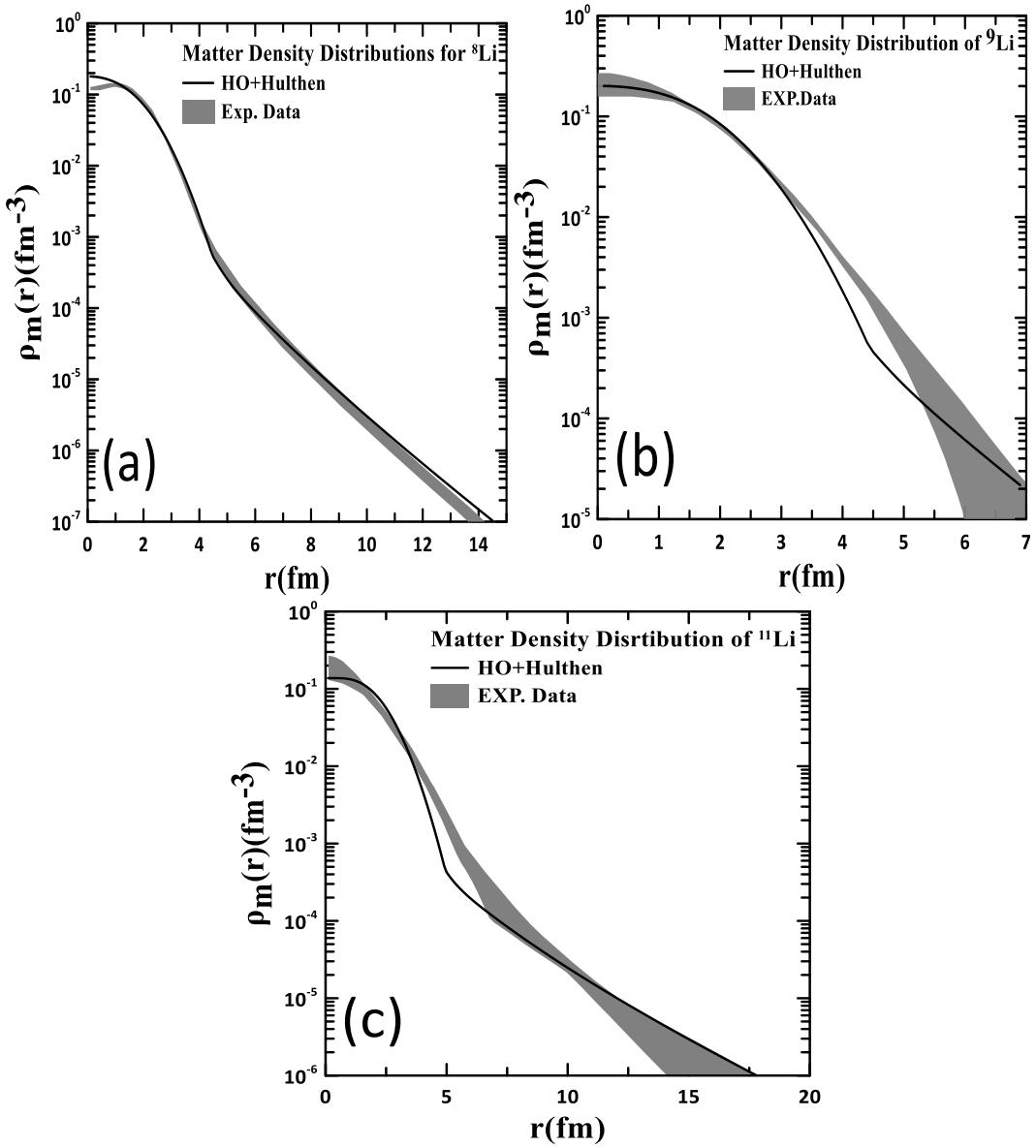

Figure 2: The solid curves represent the calculated MDDs for ^{8}Li (a), ^{9}Li (b) and ^{11}Li (c). The shaded areas extracted from the experimental data for ^{8}Li [36], for ^{9}Li [27] and for ^{11}Li [25].

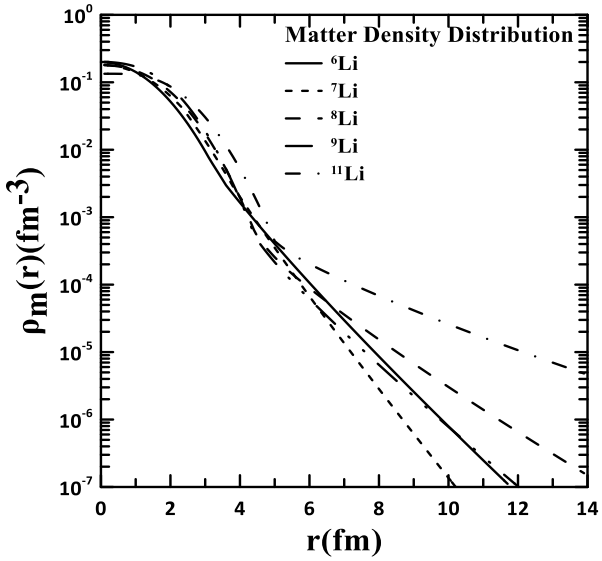

Figure 3: The computed MDDs for (^{6,7,8,9,11}Li) are displayed for comparison.

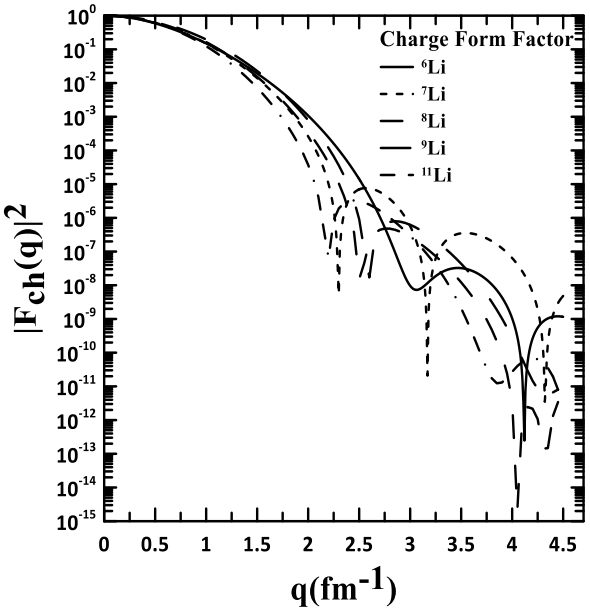

Figure 4: The calculated charge form factors for ^{9,11,12,14}Be.

Conclusions

It can be concluded that the reliance on the radial WF of Hulthen potential to calculate the bulk properties (size radii, density distributions and quadrupole moment and charge form factors) for lithium (^{6,7,8,9,11}Li) isotopes gave very good results. It was found that increasing the core radius (the matching point between HO and Hulthen) increased the calculated rms radii. The computed CDD for ^{6}Li and ^{7}Li nuclei underestimated the data at the central region; in addition, there was very good agreement with the experimental data. The decrease in the binding energy for the valence nucleon(s) led to an increase in the tail; this is attributed to the increase of the tunnelling effect. There were forward and upward shifts for the lithium isotopes except for ^{6}Li and ^{7}Li. The Bohr-Mottelson and Tassie models were used to calculate the CP contribution for ^{6}Li and ^{7}Li. The results of the previous model showed very good agreement with the experimental data.

References

[1] I. Tanihata, H. Hamagaki, O. Hashimoto, Y. Shida, and N. Yoshikawa, "Measurements of Interaction Cross Sections and Nuclear Radii in the Light p- Shell Region," *Phys. Rev. Lett.*, vol. 55, no. 24, pp. 2676-2679, 1985.

[2] I. Tanihata, H. Hamagaki, O. Hashimoto, S. Nagamiya, Y. Shida, N. Yoshikawa, O. Yamakawa, K. Sugimoto, T. Kobayashi, D. E. Greiner, N. Takahashi and Y. Nojiri, "Measurement of interaction cross sections and radii of He isotopes," *Phys. Lett. B*, vol. 160, no. 6, pp 380-384, 1985.

[3] P. Navrátil and B. R. Barrett, "Large-basis shell-model calculations for p-shell nuclei," *Phys. Rev.* C, vol. 57, pp. 3119-3128, 1998.

[4] P. Navrátil and W. Erich Ormand, "Ab initio shell model with a genuine three- nucleon force for the p-shell nuclei," *Phys. Rev.* C, vol. 68, no. 034305, pp. 1-13, 2003.

[5] P. Navrátil, E. W. Ormand C. Etienne, and C. Bertulani, "No-Core Shell Model and Reactions," *AIP Conference Proceedings*, vol. 791, pp. 32-39, 2005.

[6] R. A. Radhi, A. K. Hamoudi and A. R. Ridha, "Elastic Electron Scattering from Unstable Neutron-Rich ^{19}C Exotic Nucleus," *Iraqi Journal of Science*, vol. 54, no. 2, pp. 324-332, 2013.

[7] A. R. Ridha and Z. M. Abbas, "Study of matter density distributions, elastic charge form factors and size radii for halo 11Be, 19C and 11Li nuclei," *Iraqi Journal of Physics*, vol. 16, no. 36, pp. 29-38, 2018.

[8] A. R. Ridha, M. K. Suhayeb, "Theoretical Study of Nuclear Density Distributions and Elastic Electron Scattering form Factors for Some Halo Nuclei," *Iraqi Journal of Science*, vol. 58, no. 4B, pp. 2098-2106, 2017.

[9] S. H. Mohammed and A. R. Ridha, "Theoretical Study of the Electromagnetic Structure of Boron Isotopes Using Local Scale Transformation Technique," *Iraqi Journal of Science*, vol. 59, no. 4A, pp. 1866-1877, 2018.

[10] S. S. Odah, "Investigation of Ground Density Distributions and Charge Form Factors for 14,16,18,20,22N using Cosh Potential," *Iraqi Journal of Science*, vol. 63, no. 9, pp. 3737-3745, 2022.

[11] R. I. Noori and A. R. Ridha, "Density Distributions and Elastic Electron Scattering Form Factors of Proton-rich 8B, 17F, 17Ne, 23Al and 27P Nuclei," *Iraqi Journal of Science*, vol. 60, no. 6, pp. 1286- 1296, 2019.

[12] KG Heyde, "The Nuclear Shell Model," *Verlag Berlin Heidelberg*, 1994.

[13] G. Roger Newton, "Scattering Theory of Waves and Particles," *McGraw-Hill, New York*, pp. 282, 1966.

[14] A. Laid, J. A. Tostevin and R. C. Johanson, "Deuteron breakup effects in transfer reactions using a Weinberg state expansion method," *phys. Rev. C*, vol. 48, no. 3, pp. 1307-1317, 1993.

[15] P. J. Von Brussard and P. W. M. Glaudemans, *North-Holland, Amesterdam*, 1977.

[16] R. Arkan Ridha and M. Zaid Abbas, "Theoretical Study of Density Distributions and Size Radii of 8B and 17Ne," *Iraqi Journal of Science*, vol. 59, no. 2C, pp. 1046-1056, 2018.

[17] L. R. B. Elton, *Oxford University Press*, vol. 134, no. 3496, pp. 2092-2093, 1961.

[18] A Bohr and B R Mottelson, "Nuclear Structure," vol. 1, World Scientific, Singapore, pp. 1-9, 1998.

[19] G. Bertsch and S. F. Tsai, "How good is the collective model?" *Phys. Lett. B*, vol. 50, no. 3, pp. 319-322, 1974.

[20] A. K. Hamoudi, R. A. Radhi, A. R. Ridha, "Theoretical study of matter density distribution and elastic electron scattering form factors for the neutron-rich 22C exotic nucleus*," Iraqi. J. Phys.* (IJP), vol. 10, no. 19, pp. 25-34, 2012.

[21] H. de Vries, C. W. de Jager and C. de Vries, "Nuclear charge- density-distribution parameters from elastic electron scattering," *Atomic data and nuclear data tables*, vol. 36, no. 3, pp. 495-536, 1987.

[22] N. Stone, "Table of nuclear magnetic dipole and electric quadrupole moments," *Atomic Data Nuclear Data Tables*, vol. 90, no. 1, pp. 75-176, 2005.

[23] G. Audi, F. G. Kondev, W. J. Huang, and S. Naimi. "The NUBASE2016 evaluation of nuclear properties," *Chinese Physics C*, vol. 41, no. 3, pp. 1-138, 2017.

[24] F. G. Kondev, M. Wang, W. J. Huang, S. Naimi and G. Audi, "The NUBASE2020 evaluation of nuclear physics properties," *Chinese Physics C*, vol. 45, no. 3, pp. 1-180, 2021.

[25] T. Moriguchi, A. Ozawa, S. Ishimoto, Y. Abe, M. Fukuda, I. Hachiuma, Y. Ishibashi, Y. Ito, T. Kuboki, M. Lantz, D. Nagae, K. Namihira, D. Nishimura, T. Ohtsubo, H. Ooishi, T. Suda, H. Suzuki, T. Suzuki, M. Takechi, K. Tanaka, and T. Yamaguchi, "Density distributions of 11Li deduced from reaction cross-section measurements," *phys. Rev. C*, vol. 88, p. 024610, 2013.

[26] G. D. Alkhazov, A. A. Vorobyov, A. V. Dobrovolsky, A. G. Inglessi, G. A. Korolev, and A. V. Khanzadeev, "Investigation of the Structure of Light Exotic Nuclei by Proton Elastic Scattering in Inverse Kinematics," *Physics of Atomic Nuclei*, vol. 78, no. 3, pp: 381-386, 2015.

[27] A. V. Dobrovolsky, G. D. Alkhazov, M. N. Andronenko, A. Bauchet, P. Egelhof, S. Fritz, H. Geissel, C. Gross, A. V. Khanzadeev, G. A. Korolev, G. Kraus, A. A. Lobodenko, G. Münzenberg, M. Mutterer, S. R. Neumaier, T. Schäfer, C. Scheidenberger, D. M. Seliverstov, N. A. Timofeev, A. A. Vorobyov, V. I. Yatsoura, "Study of the nuclear matter distribution in neutron-rich Li isotopes," *Nuclear Physics A*, vol. 766, pp. 1–24, 2006.

[28] Suhel Ahmad, A. A. Usmani, and Z. A. Khan, "Matter radii of light proton-rich and neutron-rich nuclear isotopes," *phys. Rev. C*, vol. 96, pp. 1-17 2017.

[29] P. Egelhof, G.D. Alkhazov, M.N. Andronenko, A. Bauchetl, A.V. Dobrovolsky, S. Frit G.E. Gavrilov, H. GeisseP, C. Gross, A.V. Khanzadeev, G.A. Korolev, G. Kraus, A.A. Lobodenko, G. Munzenberg, M. Mutterer, S.R. Neumaier, T. Schafer C. Scheidenbergerl, D.M. Seliverstov, N.A. Timofeev, A.A. Vorobyov, and V.I. Yatsoura, "Nuclear-matter distributions of halo nuclei from elastic proton scattering in inverse kinematics," *Eur. Phys. J. A*, vol. 15, pp. 27-33, 2002.

[30] R. Sa´nchez, W. No¨rtersha¨user, G. Ewald, D. Albers, J. Behr, P. Bricault, B. A. Bushaw, A. Dax, J. Dilling, M. Dombsky, G. W. F. Drake, S. Go¨tte, R. Kirchner, H.-J. Kluge, Th. Ku¨hl, J. Lassen, C. D. P. Levy, M. R. Pearson, E. J. Prime, V. Ryjkov, A. Wojtaszek, Z.-C. Yan, and C. Zimmermann, "Nuclear Charge Radii of ^{9,11}Li: The Influence of Halo Neutrons," *Phys. Rev. Lett*., vol. 96, p. 033002, 2006.

[31] I. Tanihata, T. Kobayashi, O. Yamakawa, S. Shimoura, K. Ekuni, K. Sugimoto, N. Takahashi, T. Shimoda and H. Sato, "Measurement of interaction cross sections using isotope beams of Be and B and isospin dependence of the nuclear radii," *Phys. Lett. B*, vol. 206, p. 592, 1988.

[32] I Tanihata, T Kobayashi, T Suzuki, K Yoshlda, S. Shlmoura, K Suglmoto, K Matsuta, T Mlnamlsono, W Christie, D Olson and H Wleman, "Determination of the density distribution and the correlation of halo neutrons in ^{11}Li," *Phys. Lett. B*, vol 287, p. 307, 1992.

[33] G. C. Li, I. Sick, R. R. Whitney and M. R. Yearian, "High-energy electron scattering from ^{6}Li," Nucl. Phys. A, vol. 162, pp. 583-592. 1971.

[34] L. R. Suelzle, M. R. Yearian, H. Crannell, "Elastic Electron Scattering from Li^6 and Li^7," *Phys. Rev*., vol. 162, pp. 992-1005, 1967.

[35] J. Lichtenstadt, J. Alster, M.A. Moinester, J. Dubach, R.S. Hicks, G.A. Peterson, S. Kowalski, "High momentum transfer longitudinal and transverse form factors of the ^{7}Li ground-state doublet," *Phys. Lett. B*, vol. 219, no. 4, pp. 394-398, 1989.

[36] G. W. Fan, M. Fukuda, D. Nishimura, X. L. Cai, S. Fukuda, I. Hachiuma, C. Ichikawa, T. Izumikawa, M. Kanazawa, A. Kitagawa, T. Kuboki, M. Lantz, M. Mihara, M. Nagashima, K. Namihira, Y. Ohkuma, T. Ohtsubo, Zhongzhou Ren, S. Sato, Z. Q. Sheng, M. Sugiyama, S. Suzuki, T. Suzuki, M. Takechi, T. Yamaguchi, and W. Xu, "Density distribution of 8Li and 8B and capture reaction at low energy," *phys. Rev. C*, vol. 91, p. 014614, 2015.